Acta Biomaterialia 105 (2020) 78–86

Contents lists available at ScienceDirect

Acta Biomaterialia

journal homepage: www.elsevier.com/locate/actbio

Full length article

Myofibroblast activation in synthetic fibrous matrices composed of dextran vinyl sulfone

Christopher D. Davidson[a], Danica Kristen P. Jayco[a], Daniel L. Matera[b], Samuel J. DePalma[a], Harrison L. Hiraki[a], William Y. Wang[a], Brendon M. Baker[a,*]

[a] Department of Biomedical Engineering, University of Michigan, Ann Arbor, MI 48109, United States
[b] Department of Chemical Engineering, University of Michigan, Ann Arbor, MI 48109, United States

ARTICLE INFO

Article history:
Received 22 October 2019
Revised 18 December 2019
Accepted 8 January 2020
Available online 13 January 2020

Keywords:
Electrospinning
Nanofibers
Extracellular matrix
Microenvironment
Cell culture substrates
Dextran vinyl sulfone
Mechanical characterization
Cell adhesion
Mechanosensing
Fibroblast
Myofibroblast

ABSTRACT

Mechanical interactions between fibroblasts and their surrounding extracellular matrix (ECM) guide fundamental behaviors such as spreading, migration, and proliferation that underlie disease pathogenesis. The challenges of studying ECM mechanics *in vivo* have motivated the development of *in vitro* models of the fibrous ECM in which fibroblasts reside. Natural materials such as collagen hydrogels bear structural and biochemical resemblance to stromal ECM, but mechanistic studies in these settings are often confounded by cell-mediated material degradation and the lack of structural and mechanical tunability. Here, we established a new material system composed of electrospun dextran vinyl sulfone (DexVS) polymeric fibers. These fibrous matrices exhibit mechanical tunability at both the single fiber (80–340 MPa) and bulk matrix (0.77–11.03 kPa) level, as well as long-term stability in mechanical properties over a two-week period. Cell adhesion to these matrices can be either user-defined by functionalizing synthetic fibers with thiolated adhesive peptides or methacrylated heparin to sequester cell-derived ECM proteins. We utilized DexVS fibrous matrices to investigate the role of matrix mechanics on the activation of fibroblasts into myofibroblasts, a key step of the fibrotic progression. In contrast to previous findings with non-fibrous hydrogel substrates, we find that fibroblasts in soft and deformable matrices exhibit increased spreading, focal adhesion formation, proliferation, and myofibroblast activation as compared to cells on stiffer matrices with equivalent starting architecture.

Statement of significance

Cellular mechanosensing of fibrillar extracellular matrices plays a critical role in homeostasis and disease progression in stromal connective tissue. Here, we established a new material system composed of electrospun dextran vinyl sulfone polymeric fibers. These matrices exhibit architectural, mechanical, and biochemical tunability to accurately model diverse tissue microenvironments found in the body. In contrast to previous observations with non-fibrous hydrogels, we find that fibroblasts in soft and deformable fibrous matrices exhibit increased spreading and focal adhesion formation as compared to those in stiffer matrices with equivalent architecture. We also investigated the role of matrix stiffness on myofibroblast activation, a critical step in the fibrotic cascade, and find that low stiffness matrices promote increased myofibroblast activation.

1. Introduction

Interactions with the extracellular matrix (ECM) guide fundamental cell behaviors including spreading, migration, and proliferation, and thus play an important role in connective tissue homeostasis, repair processes, and pathogenesis [1,2]. Due to the diversity in ECM structure and mechanics throughout various tissues, cells are exposed to a wide range of physical cues and must appro-

* Corresponding author at: Department of Biomedical Engineering, University of Michigan, 2174 Lurie BME Building, 1101 Beal Avenue, Ann Arbor, MI 48109, United States.
E-mail address: bambren@umich.edu (B.M. Baker).

https://doi.org/10.1016/j.actbio.2020.01.009
1742-7061/

priately sense and respond to these signals over time to properly maintain tissue form and function [3]. Cells mechanically engage their physical microenvironment through integrin-based adhesion complexes, or focal adhesions. These mechanoresponsive signaling hubs link the ECM to the actin cytoskeleton, allowing cells to probe and respond to the physical attributes of their surroundings [4–6]. Significant recent work has demonstrated the importance of matrix elastic modulus in regulating focal adhesions and cell behavior [7–10], but cells have also been shown to sense a wide range of other physical properties including topography [11], porosity [12], and viscoelasticity [13].

It has long been known that abnormal tissue mechanics and consequent altered cellular mechanoresponse is a component of many diseases [3]. However, elucidating the role of mechanics during disease pathogenesis *in vivo* has proven difficult due to the limited ability to experimentally modulate properties of native tissues. Thus, many have turned to *in vitro* models to study how ECM physical properties regulate cell behavior [14]. Natural fibrous biomaterials, such as collagen and fibrin hydrogels, are used extensively due to their structural and biochemical similarity to native connective tissues [15,16]. However, mechanistic studies in these settings are confounded by the rapid production of cell-secreted matrix, impact of cell-mediated ECM proteolysis, and lack of orthogonal control over structural and mechanical characteristics [14]. Furthermore, the limited stability of these hydrogel matrices due to degradation and/or contraction can hinder long term culture (depending on protein density and cell type) [17,18]. Conversely, synthetic hydrogels, such as polyacrylamide or poly(ethylene glycol) (PEG), offer control over matrix elastic modulus, ligand presentation, and degradability, making them ideal for mechanistic studies [14]. However, synthetic hydrogels are nanoporous, mechanically isotropic and homogeneous at the cell-scale. This class of materials lacks the discrete fibrous structure and resulting complex mechanical behavior of native collagen-rich connective tissues.

Electrospinning has been extensively used to fabricate synthetic fibrous scaffolds that mimic the structure of native tissue ECMs [19,20]. A simple and versatile approach, electrospinning can produce scaffolds from a variety of synthetic and natural polymers that facilitate cell attachment and viability [21]. By modulating the electrospinning process and solution parameters, electrospun scaffolds have shown high levels of control over matrix topography, such as fiber diameter and pore size. Recent work from our lab has combined the electrospinning technique with photo-crosslinkable polymer chemistry to generate matrices composed of methacrylated dextran (DexMA) fibers with stiffness tuned via light exposure [22]. While the high degree of control over ECM architectural and mechanical properties has shed insight on how cells interpret the physical properties of fibrous matrices during cell spreading [22], migration [23], and multicellular assembly [24], ester hydrolysis mediated degradation of crosslinked DexMA networks has prevented cell studies longer than a few days in this setting.

Fibrosis is one context where an improved understanding of longer-term mechanosensing in fibrous microenvironments would be invaluable. Fibrosis is associated with numerous heart, lung, and vascular diseases, and is implicated in an estimated 45% of all deaths in the developed world [25,26]. The principal cells that drive this disease process are myofibroblasts (MFs), characterized by heightened rates of proliferation and the expression of alpha smooth muscle actin (α-SMA) [25,27,28]. These cells gradually contribute to organ stiffening, contraction, and eventual failure via excessive ECM synthesis, crosslinking, and application of contractile forces. Profibrotic microenvironmental cues in stromal connective tissues are known to activate cells residing within the tissue or recruited from circulation into MFs [29–31]. While our understanding of the transition from normal to fibrotic tissue is still incomplete, it is understood that profibrotic soluble signals such as TGF-β1 are potentiated by matrix mechanical cues [32–36]. For example, experiments varying the Young's modulus of polyacrylamide, PEG, and hyaluronic acid hydrogel surfaces have demonstrated that substrates with higher stiffness promote fibroblast MF activation (measured via expression levels of α-SMA) as compared to low modulus substrates [35–39]. However, as these gel surfaces lack fibrillar structure and possess limited potential for cellular remodeling as observed during fibrosis, there remains a need for fibrous materials that are mechanically well-defined, tunable, and stable over long-term culture to provide insight into the dynamics of ECM mechanics throughout this critical disease process.

Here, we aimed to develop a synthetic fibrous matrix resistant to degradation in order to study long-term cellular behavior in the context of MF activation from normal fibroblasts. We synthesized and electrospun photocrosslinkable dextran vinyl sulfone (DexVS) fibrous matrices that are resistant to hydrolytic degradation and therefore mechanically stable over longer-term cell culture. DexVS matrices have controllable architecture through modulation of electrospinning parameters and are mechanically tunable at both the single fiber and matrix levels. Furthermore, the dextran backbone results in protein-resistant fibers that can be functionalized with thiolated peptides via Michael-type addition or with methacrylated heparin to free vinyl sulfone groups to allow for cell adhesion and matrix remodeling, respectively. Examining cell behavior on DexVS matrices as a function of matrix stiffness, we find that fibroblasts cultured on soft matrices actively displace and bundle matrix fibers and have larger spread area and focal adhesion area than fibroblasts on stiff, non-deformable matrices. Additionally, contrary to previous studies on 2D elastic hydrogels, we observed higher levels of MF activation when fibroblasts are cultured on soft rather than stiff fibrous matrices in the presence of the pro-fibrotic soluble factor TGF-β1.

2. Materials and methods

2.1. Reagents

All reagents were purchased from Sigma Aldrich and used as received, unless otherwise stated.

2.2. Cell culture

Normal human lung fibroblasts (NHLFs, University of Michigan Central Biorepository, Ann Arbor, MI) were cultured in DMEM containing 1% penicillin/streptomycin, L-glutamine, and 10% fetal bovine serum (basal medium). Cells were cultured at 37 °C and 5% CO_2. NHLFs between passages four and ten were used for experiments.

2.3. DexVS synthesis

Dextran was reacted with divinyl sulfone following a previously described procedure [40]. Briefly, dextran (5 g) was dissolved in 250 mL of sodium hydroxide (100 mM) solution on a stir plate at 300 rpm before addition of divinyl sulfone (12.5 mL). The reaction proceeded for 3.5 min before termination by addition of 2.5 mL hydrochloric acid (12 M). The product was dialyzed against milli-Q water for 3 days and then lyophilized. DexVS was characterized by ^{1}H NMR and a vinyl sulfone/dextran repeat unit ratio of 0.66 was determined (Fig. S1).

2.4. Fibrous matrix fabrication

DexVS was dissolved at 0.7 g mL^{-1} in a 1:1 mixture of milli-Q water and dimethylformamide with 0.6% (w/v) lithium phenyl-2,4,6-trimethylbenzoylphosphinate (LAP; Colorado Photopolymer

Solutions, Boulder, CO) photoinitiator, 2.5% (v/v) methacrylated rhodamine (25 mM; Polysciences, Inc., Warrington, PA), and 5.0% (v/v) glycidyl methacrylate. Electrospinning was accomplished with a custom set-up consisting of a high-voltage power supply (Gamma High Voltage Research, Ormond Beach, FL), syringe pump (KD Scientific, Holliston, MA), and a grounded copper collecting surface enclosed within an environmental chamber held at room temperature and 35% relative humidity (Terra Universal, Fullerton, CA). Electrospinning of DexVS solution was performed at a flow rate of 0.2 mL h^{-1}, voltage of 7.0 kV, and gap distance of 7 cm. To induce fiber alignment, fibers were electrospun at a voltage of 4.0 kV onto a collecting surface of oppositely charged (−3.0 kV) parallel electrodes with varying separation distance to control alignment. After electrospinning, fibers were stabilized by primary crosslinking under UV light (100 mW cm^{-2}) for 120 s, hydrated in varying concentrations of LAP solution, and then exposed again to UV light (100 mW cm^{-2}) for varying durations. Fibers were collected on poly(dimethylsiloxane) (PDMS; Dow Silicones Corporation, Midland, MI) arrays of circular wells produced by soft lithography as previously described [22]. Briefly, silicon wafer masters possessing SU-8 photoresist (Microchem, Westborough, MA) were produced by standard photolithography and used to generate PDMS stamps. Following silanization with trichloro(1H,1H,2H,2H-perfluorooctyl)silane, stamps were used to emboss uncured PDMS onto oxygen plasma-treated coverslips. Well arrays were methacrylated with vapor-phase silanization of 3-(trimethoxysilyl)propyl methacrylate in a vacuum oven at 60 °C for at least 6 h to promote fiber adhesion to PDMS.

2.5. Mechanical testing

To determine the tensile mechanical properties of individual fibers, three-point bending tests were performed using a Nanosurf FlexBio atomic force microscope (AFM; Nanosurf, Liestal, Switzerland). Single fibers were collected onto microfabricated PDMS troughs (200 µm tall × 200 µm wide) by electrospinning for short durations (1 s). Fibers were hydrated and crosslinked to varying degrees by LAP concentration and UV light exposure as above and deformed by an AFM tip (0.032 N m^{-1}) loaded with a 35 µm diameter bead positioned centrally along the fiber's length. Young's modulus was calculated from the resulting load-displacement curves using known equations for a cylindrical rod undergoing three-point bending with fixed boundaries [41,42]. To determine the Young's modulus of suspended DexVS fibrous matrices, microindentation testing with a rigid cylinder was performed on a commercial CellScale Microsquisher (CellScale, Waterloo, Ontario). Cylinders (1 mm diameter, 0.5 mm tall) of SU-8 photoresist were microfabricated and affixed to pure tungsten filaments (0.156 mm diameter, 59.6 mm length). Samples were indented to a depth of up to 200 µm at an indentation speed of 2 µm s^{-1}. As previously described [22], Young's modulus was approximated assuming the material behaves as an elastic membrane using the following equation:

$$F = \frac{Et\pi\delta^3\left(r_o^2 - r_i^2\right)}{2(r_o - r_i)^4(1-\nu)}$$

where t is the membrane thickness (8.68 µm, as determined by confocal microscopy; Fig. S2), r_o is the membrane radius (1 mm), r_i is the indenter radius (0.5 mm), ν is the Poisson ratio (0.5), F is the indentation force, δ is the indentation depth, and E is Young's modulus.

2.6. RGD functionalization and seeding on DexVS matrices

DexVS fibers were functionalized with the cell adhesive peptide cyclized [Arg-Gly-Asp-D-Phe-Lys(Cys)] (cRGD; Peptides International, Louisville, KY) via Michael-type addition to available vinyl sulfone groups to facilitate cell attachment. Briefly, the peptide was dissolved at 100 µM (unless otherwise stated) in milli-Q water containing HEPES (50 mm), phenol red (10 µg mL^{-1}), and 1M NaOH to adjust the pH to 8.0. A 400 µL volume of this solution was added to each substrate and incubated for 30 min at room temperature. Following cRGD functionalization, substrates were rinsed 2x with PBS before cell seeding. NHLFs were trypsinized, centrifuged and resuspended in basal medium, and seeded at 10^4 cells cm^{-2}.

2.7. Passive adsorption of proteins to DexVS matrices

Type I rat tail collagen and human fibronectin (Corning Incorporated, Corning, NY) were each diluted in PBS at 100 µg mL^{-1}. A 400 µL volume of either collagen solution, fibronectin solution, or fetal bovine serum (Atlanta Biologics, Flowery Branch, GA) was added to each substrate and incubated for 30 min at room temperature. Following protein adsorption, substrates were rinsed 3x with PBS before cell seeding.

2.8. HepMA synthesis and functionalization

Heparin sodium salt was reacted with methacrylic anhydride following previously described procedures [43,44]. Briefly, heparin sodium salt (500 mg) was dissolved in 50 mL PBS under vigorous stirring before addition of methacrylic anhydride (99.3 mL). The reaction was kept under constant stirring at 4 °C for 24 h. NaOH (1 N) was added every hour for the first 6 h to maintain a solution pH of 8. The product was dialyzed against milli-Q water for 3 days and then lyophilized. Heparin methacrylate (HepMA) was dissolved in LAP solution at 2.5% (w/v). Fibers were simultaneously crosslinked and functionalized in this solution via exposure to UV light (100 mW cm^{-2}).

2.9. Myofibroblast induction

NHLFs were seeded and allowed to adhere for 24 h. Following cell attachment, basal media was supplemented with TGF-β1 (10 ng mL^{-1}) and cultured for an additional 6 days. Media was replaced every 2 days.

2.10. Fluorescent staining and microscopy

NHLFs on DexVS fibers were first fixed in 4% paraformaldehyde for 10 min at room temperature. Alternatively, to extract cytoplasmic vinculin, samples were simultaneously fixed and permeabilized in 2% paraformaldehyde in a buffer containing 1,4-piperazinediethanesulfonic acid (PIPES, 0.1 M), ethylene glycol-bis(2-aminoethylether)-N,N,N',N'-tetraacetic acid (EGTA, 1 mM), magnesium sulfate (1 mM), poly(ethylene glycol) (4 % w/v), and triton X-100 (1% v/v) for 10 min at room temperature. To stabilize the fibers for processing and long-term storage, DexVS samples were crosslinked in 2 mL LAP solution (1.0% w/v) and exposed to UV light (100 mW cm^{-2}) for 30 s. To stain the actin cytoskeleton and nuclei, cells were permeabilized in PBS solution containing Triton X-100 (5% v/v), sucrose (10% w/v), and magnesium chloride (0.6% w/v), and simultaneously blocked in 1% (w/v) bovine serum albumin and stained with phalloidin and DAPI. For immunostaining, samples were permeabilized, blocked for 1 h in 1% (w/v) bovine serum albumin, and incubated with mouse monoclonal anti-vinculin antibody (1:1000, Sigma #V9264), mouse monoclonal anti-fibronectin antibody (1:2000, Sigma #F6140), or mouse monoclonal anti-α-SMA (1:2000, Sigma #A2547) followed by secondary antibody (1:1000, Life Technologies #A21236) for 1 h each at room temperature with 3x PBS washes in between. For proliferation studies, EdU labelling was performed following the

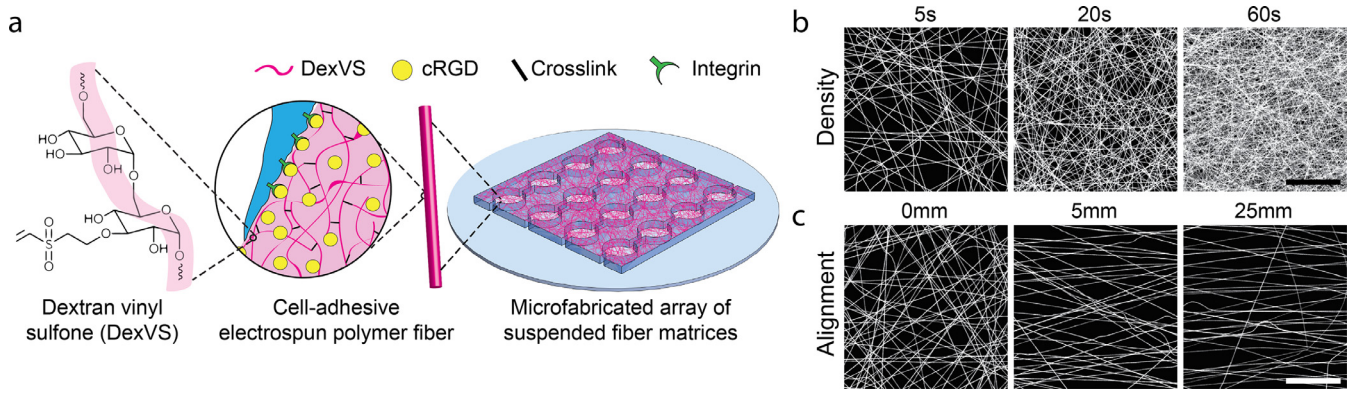

Fig. 1. DexVS fibrous matrices with tunable architectural features. (a) Schematic of microfabricated PDMS multi-well substrate possessing a 4 × 4 array of wells, each supporting a suspended matrix of DexVS fibers coupled with cRGD to facilitate cell adhesion. Through modulation of the electrospinning fabrication process, networks were fabricated with varying (b) fiber density via fiber collection duration and (c) alignment via controlling the separation distance between two parallel electrodes at the collecting surface. Scale bars: 50 μm.

manufacturer's protocol (Click-iT EdU, Life Technologies, Carlsbad, CA). Fixed samples were imaged on a Zeiss LSM 800 laser scanning confocal microscope (Zeiss, Oberkochen, Germany). For cell studies, only cells in the central region of each suspended matrix (2 mm diameter) were imaged. Unless otherwise specified, images are presented as maximum intensity projections. Fluorescent images were processed and quantified via custom Matlab scripts.

2.11. Statistics

Statistical significance was determined by one-way analysis of variance (ANOVA) with post-hoc analysis (Tukey test) or Student's t-test where appropriate, with significance indicated by $p < 0.05$. Sample size is indicated within corresponding figure legends and all data are presented as mean ± standard deviation.

3. Results and discussion

3.1. DexVS matrix fabrication and mechanical characterization

To model the fibrous microstructure of collagenous stromal tissue where fibrosis begins, we devised a synthetic matrix composed of assemblies of electrospun DexVS polymeric fibers (Fig. 1a). The polysaccharide dextran was chosen as a polymer backbone given its abundance of hydroxyl groups for modification and previous literature indicating amenability to electrospinning [45–47]. Furthermore, materials composed of crosslinked dextran have been shown to be resistant to protein adsorption, thereby allowing user-defined control over cell-adhesive ligand type and concentration [48]. We have previously employed dextran functionalized with methacrylates (DexMA) to investigate short term (less than 2 days) cell response in fibrous matrices with controllable biophysical and biochemical properties [22]. Over longer durations of cell culture, however, deviations in pH due to the metabolic activity of cultured cells promote ester hydrolysis-mediated degradation of these matrices. To engineer matrices that permit long-term cell culture, we employed vinyl sulfones due to their reactivity, stability after functionalization, and resultant crosslinks lacking hydrolytically cleavable ester bonds [49]. Like methacrylates, vinyl sulfones enable modular material design through functionalization and crosslinking via Michael-type addition or photopolymerization in the presence of photoinitiator.

Matrices were fabricated by electrospinning a solution of DexVS and LAP photoinitiator onto PDMS collection substrates such that fibers were suspended over an array of microfabricated wells (Ø = 2 mm) (Fig. 1a). Thus, cells that adhere within suspended matrices above microwell regions sense the physical cues defined by the architecture and mechanical properties of the fibrous matrix and its anchorage at microwell edges, without the influence of a rigid underlying support surface. As demonstrated previously with DexMA [22], various architectural features of DexVS matrices can be tuned by modulating fabrication parameters. The density and alignment of fibers within matrices were controlled by modulating electrospinning duration and the distance between parallel collecting electrodes, respectively (Fig. 1b,c). DexVS fiber diameter and overall matrix thickness were measured via confocal microscopy to be approximately 1.02 ± 0.15 μm and 8.68 ± 0.73 μm, respectively (Fig. S2).

Beyond architectural features, the stiffness of individual DexVS fibers can be tuned by varying the crosslinking density of the polymer network composing each fiber. Exposure to UV light immediately after electrospinning renders crosslinked fibers water insoluble, allowing a second phase of LAP initiated crosslinking following sample hydration. We hypothesized control over either the duration of UV light exposure or LAP concentration during this second phase of crosslinking could controllably define the stiffness of individual fibers. To directly test this, we determined the Young's moduli of individual fibers via microscale three-point bending tests using AFM (Fig. 2a). Young's modulus of individual fibers was tunable between 80 and 340 MPa and proved more sensitive to LAP concentration than UV exposure time (Fig. 2b,c). These modulus values are within the range of reported values for various fibrous biopolymers such as fibrin or collagen (1-75,000 MPa) [41,50,51].

In addition to mechanically characterizing individual fibers, we also measured stiffness of suspended assemblies of fibers (hereafter referred to as matrix stiffness). We performed microindentation tests of suspended DexVS matrices with a rigid cylindrical indenter to estimate the Young's modulus (Fig. 3a). In agreement with single fiber measurements, increasing both UV exposure time and LAP concentration led to subsequent increases in matrix stiffness. Specifically, we were able to tune the Young's modulus between 0.77 and 11.03 kPa (Fig. 3b,c), allowing for precise control of matrix stiffness over a physiologically relevant range. Additionally, we found that the matrix Young's modulus scales linearly as a function of fiber Young's modulus (Fig. 4a).

To confirm that photocrosslinked DexVS matrices are resistant to ester hydrolysis in conditions relevant to cell culture (Fig. 4b), we performed matrix mechanical testing of substrates incubated in basal media for up to two weeks. No change in Young's modulus was observed over this time period, indicating that DexVS matrices retain mechanical integrity over time in serum-containing media (Fig. 4c). In contrast, DexMA matrices with crosslinks possessing ester bonds (Fig. 4b) revealed evidence of hydrolysis-mediated degradation as marked by gradual reduction in matrix stiffness

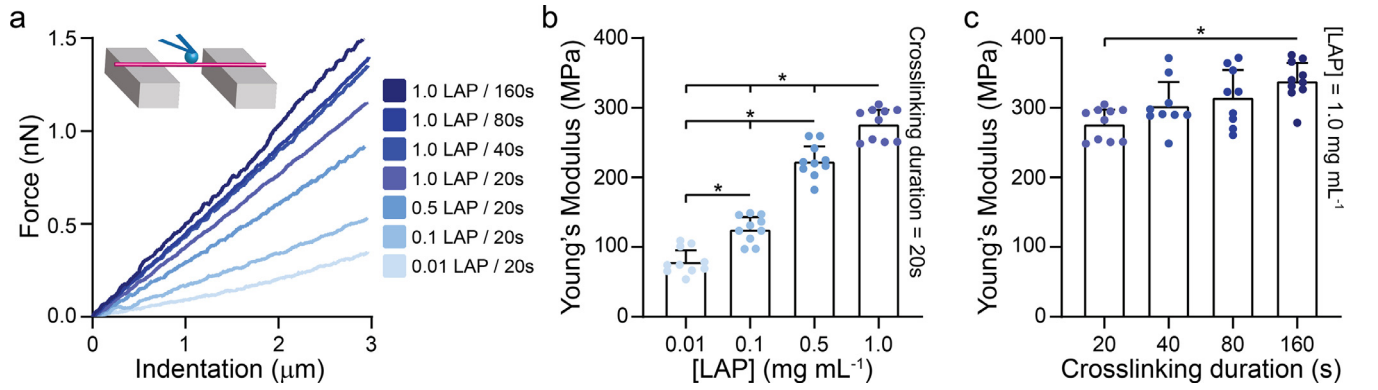

Fig. 2. Mechanical characterization of single DexVS fibers by AFM three-point bending. (a) Force response as a function of indentation depth of DexVS fibers exposed to variable crosslinking conditions. Respective Young's modulus values for DexVS fibers crosslinked with (b) varying LAP concentration for 20 s, and (c) varying crosslinking time in 1.0 mg mL^{-1} LAP. All data presented as mean ± std; n ≥ 9; * $p \leq 0.05$.

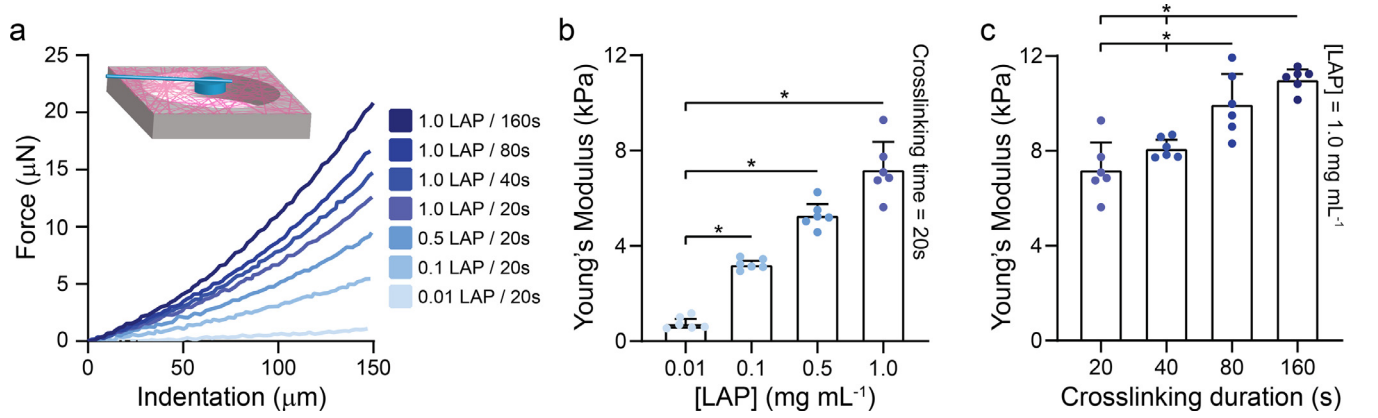

Fig. 3. Mechanical characterization of suspended DexVS matrices by microindentation with a cylindrical indenter affixed a calibrated cantilever. (a) Force response as a function of indentation depth of DexVS matrices exposed to variable crosslinking conditions. Respective Young's modulus values for DexVS matrices crosslinked with (b) varying LAP concentration for 20 s, and (c) varying crosslinking time in 1.0 mg mL^{-1} LAP. All data presented as mean ± std; $n = 6$; * $p \leq 0.05$.

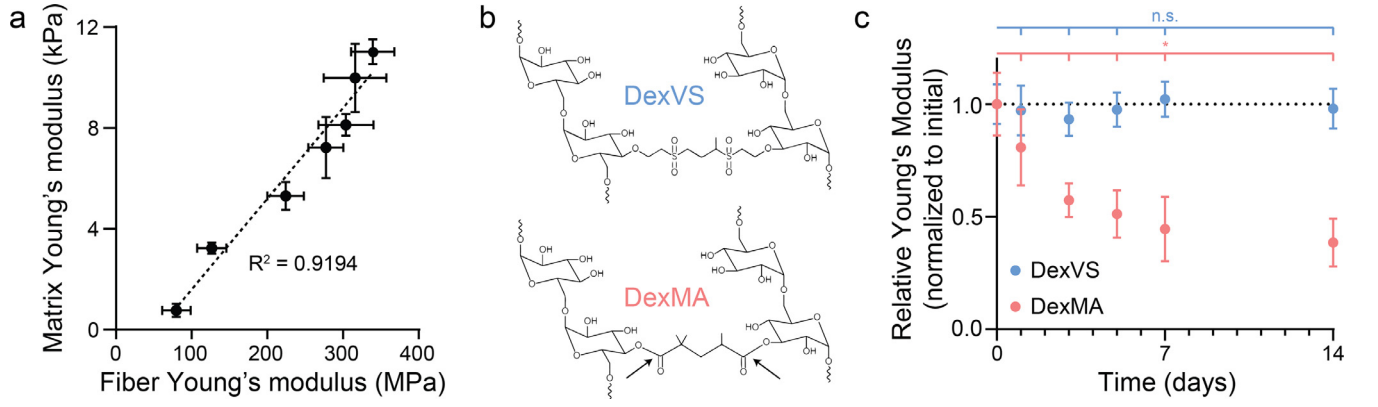

Fig. 4. Multi-scale and time-dependent mechanical characterization of DexVS matrices. (a) Matrix Young's modulus as a function of single fiber Young's modulus at variable crosslinking conditions. (b) Chemical schematic of crosslinked DexVS and DexMA. Arrows indicate ester bonds susceptible to hydrolysis. (c) Bulk Young's modulus of DexVS and DexMA matrices as a function of incubation time in basal medium for up to two weeks. All data presented as mean ± std; $n \geq 6$; * $p \leq 0.05$.

over time (Fig. 4c). DexMA matrices ultimately exhibited a 62.6% decrease from initial Young's modulus after two weeks in culture conditions.

3.2. DexVS functionalization to enable user- or cell-defined adhesion

To study cell behavior on DexVS fibrous matrices, we first functionalized fibers with a cyclized RGD peptide (cRGD) via Michael-type addition to remaining free vinyl sulfones. Fibroblasts were seeded on stiff matrices (E = 11.03 kPa) coupled with cRGD and negligible cell death was noted following overnight culture (Fig. S3). Cell attachment and spreading proved highly sensitive to the coupling concentration of cRGD, with limited cell attachment noted in the absence of adhesive ligand functionalization (Fig. 5a,b). As cell attachment and spreading were maximal at 100 μM, this concentration was utilized for all subsequent studies (Fig. 5b, Fig. S4). Furthermore, we next aimed to confirm that DexVS matrices do not passively adsorb serum-borne ECM proteins, as this could lead to confounding or uncharacterized effects on cell mechanosensing and behavior. Matrices soaked in collagen, fibronectin, or fetal bovine serum without cRGD functionalization demonstrated limited NHLF attachment

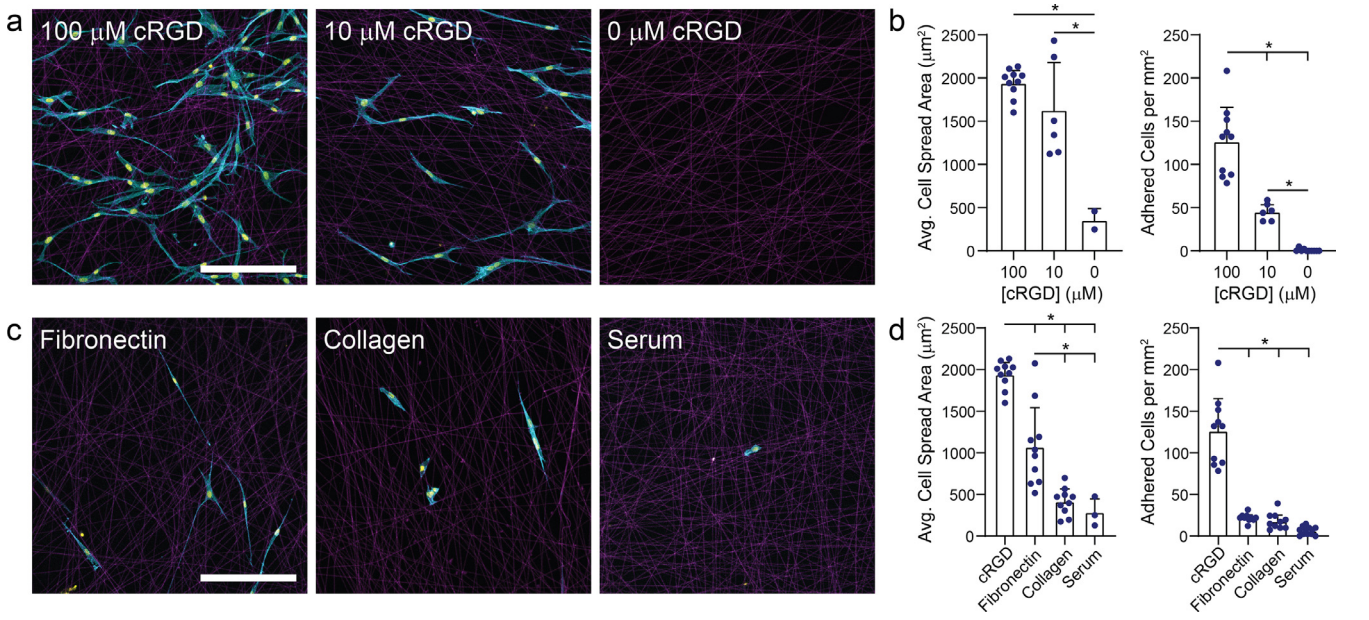

Fig. 5. DexVS functionalization with cell-adhesive peptides and passive adsorption of proteins. Confocal fluorescent images of NHLFs cultured on DexVS matrices functionalized with (a) variable cRGD concentrations and (c) soaked in fibronectin (100 μg mL^{-1}), collagen (100 μg mL^{-1}), and fetal bovine serum; actin (cyan), DexVS fibers (magenta), nuclei (yellow). Average cell spread area and number of adhered cells as a function of (b) cRGD concentration and (d) protein functionalization. Scale bars: 200 μm. All data presented as mean ± std; $n \geq 6$; * $p < 0.05$. (For interpretation of the references to color in this figure legend, the reader is referred to the web version of this article.)

and lower levels of spreading as compared to fibers functionalized with cRGD (Fig. 5c,d). These results indicate that DexVS does not allow passive adsorption of proteins, but instead requires functionalization with cysteine-terminated ligands to facilitate cell attachment.

User-defined control over adhesive ligand type and density can be beneficial for mechanistic studies of short-term processes such as cell spreading. However, during longer-term biological processes or in native tissue settings, cell-ECM interactions are bidirectional; cells not only receive physical and biochemical signals from the ECM, but also reciprocally alter encoded signals through modification of the ECM [52]. Heparin sulfate proteoglycans found ubiquitously throughout all tissues bind a plethora of cell secreted ECM proteins and growth factors for subsequent presentation to cells [53,54]. To imbue protein adsorption-resistant DexVS matrices with the ability to actively bind cell-secreted matrix components, we synthesized heparin methacrylate (HepMA) and functionalized matrices with this structural analog to heparan sulfate. HepMA was covalently conjugated into the polymer network composing DexVS fibers through radical-initiated covalent crosslinks formed between methacrylate and vinyl sulfone groups. To examine the effect of heparin incorporation on cell-secreted ECM sequestration, we seeded NHLFs on cRGD functionalized DexVS matrices with or without HepMA functionalization and stained for fibronectin (Fig. 6a). HepMA functionalization corresponded to significantly more fibronectin bound to synthetic fibers as evident by higher fluorescence intensity than controls (Fig. 6b). No difference in fibronectin staining intensity was noted between soft (E = 0.77 kPa) and stiff (E = 11.03 kPa) HepMA functionalized matrices (Fig. 6b). These results demonstrate an additional means to facilitate cell adhesion to DexVS matrices, where addition of heparin actively sequesters cell-generated ECM components, such as fibronectin, to the cellular microenvironment.

3.3. Effect of DexVS fibrous matrix stiffness on cell behavior

While cellular mechanosensing of the fibrillar microenvironment plays a critical role in tissue homeostasis and disease progression [1–3], many *in vitro* studies of mechanosensing examine cells plated on flat elastic hydrogel substrates lacking fibrous topography. Recent efforts, however, have sought to compare the cell response to stiffness in fibrous versus elastic hydrogel settings. These studies suggest disparate trends in human mesenchymal stem cell behavior as a function of matrix stiffness in discrete fibrous and continuous hydrogel settings [22,55]. Given these observations, we next aimed to examine shorter-term (<1 day) mechanosensing behaviors during NHLF adhesion and spreading on DexVS matrices as a function of matrix stiffness.

Previous studies seeding cells on the surface of non-fibrous hydrogel substrates have demonstrated that cell spreading (as measured by steady-state spread area) consistently increases with matrix stiffness [22,56,57]. In contrast, we observed a modest decrease in cell spread area with increasing fibrous matrix stiffness (Fig. 7a,d). In soft matrices, traction forces generated by NHLFs deformed the matrix, recruiting fibers directly beneath the cell body (Fig. 7b). Stiff matrices, however, proved too rigid to be deformed by cell forces. We also immunostained for vinculin, a mechanosensitive adhesion protein, to directly examine cell adhesion to the DexVS fibers (Fig. 7c). Previous work from our lab showed that fiber recruitment and densification in DexMA fibrous matrices increases local ligand concentration and correlates with an increase in human mesenchymal stem cell spread area and focal adhesion number [22]. Here, we observed similar results with NHLFs on DexVS matrices where soft, deformable matrices led to a significant increase in focal adhesion area as compared to stiff, non-deformable matrices (Fig. 7d).

These results are consistent with previous observations of short term, single cell mechanosensing events on fibrous matrices [22]. However, diseases driven by progressive changes to ECM mechanics typically involve a population or multiple populations of cells that interact bidirectionally with their surroundings over a longer span of time. During fibrosis, for instance, fibroblasts in response to biochemical and biophysical cues differentiate into MFs that excessively synthesize ECM and exert contractile forces to cause tissue contracture, stiffening, and eventual organ failure. To better understand the microenvironmental cues that promote MF activation, many have utilized 2D hydrogel substrates to examine the effect of bulk matrix stiffness. These studies revealed that substrate stiff-

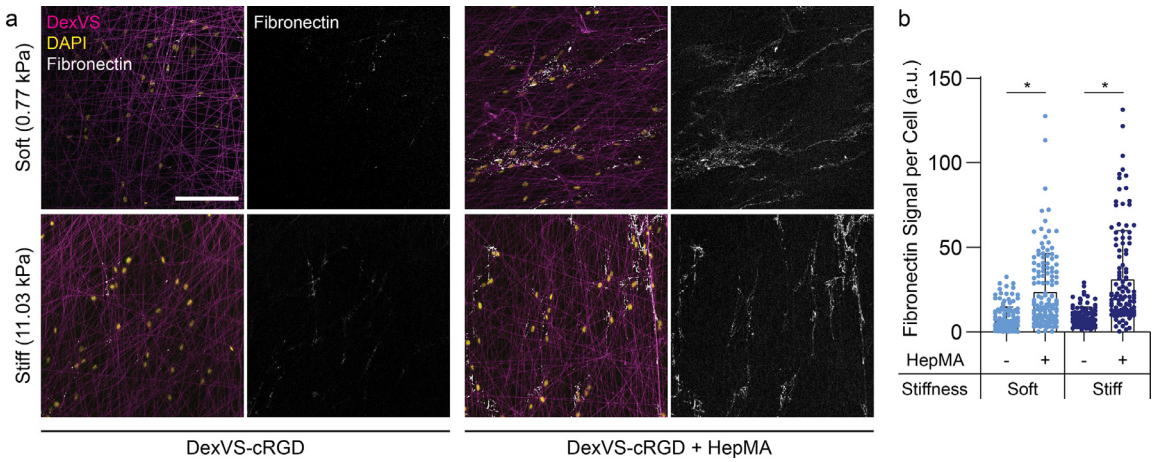

Fig. 6. HepMA functionalization increases binding of cell-secreted fibronectin to DexVS fibers. (a) Confocal fluorescent images of fibronectin (white), DexVS fibers (magenta), and nuclei (yellow). (b) Quantification of fibronectin signal per cell as a function of matrix stiffness and HepMA functionalization. Scale bar: 200 μm. All data presented as mean ± std; $n \geq 104$; * $p < 0.05$. (For interpretation of the references to color in this figure legend, the reader is referred to the web version of this article.)

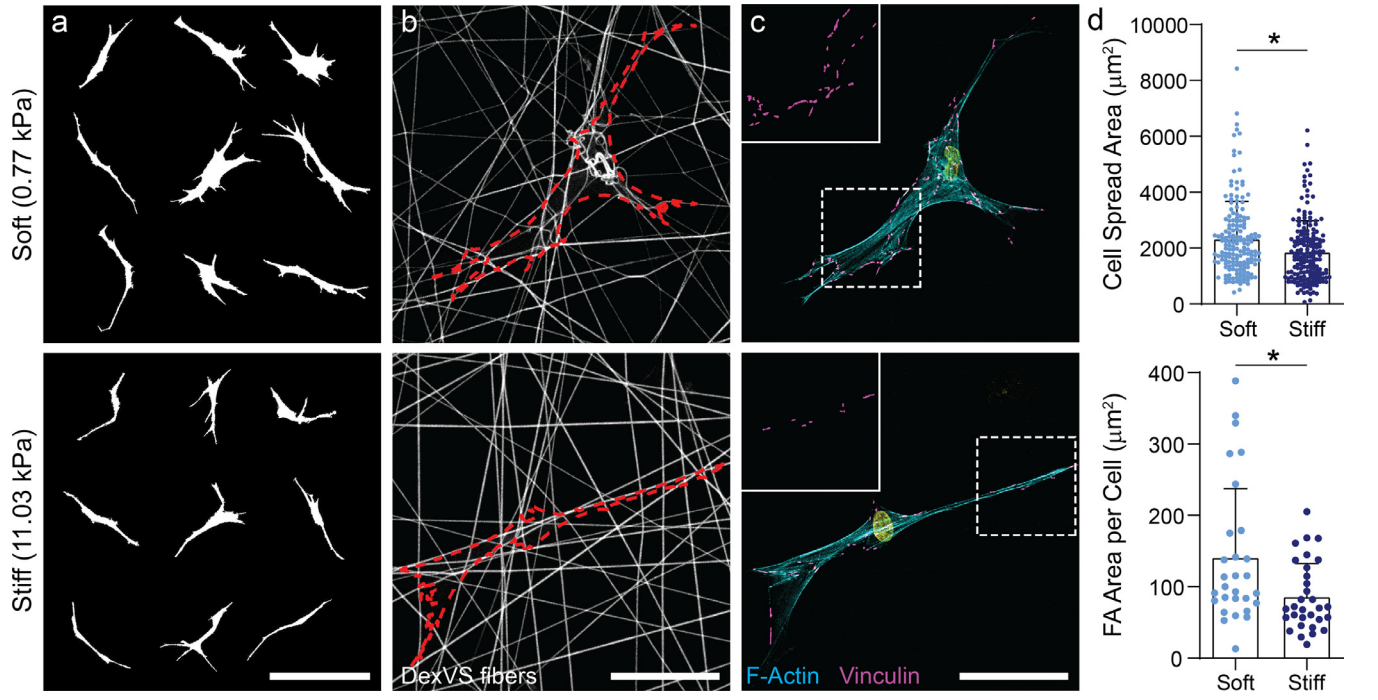

Fig. 7. Soft, deformable DexVS matrices promote increased cell spreading and focal adhesion formation. (a) Cell outlines of nine representative cells. Scale bar: 200 μm. (b) Confocal fluorescent image of rhodamine-labeled DexVS fibers with cell outline shown in red. Scale bar: 100 μm. (c) Confocal fluorescent image of phalloidin-stained NHLFs (cyan) and vinculin (magenta, top left inset). Scale bar: 100 μm. (d) Quantification of cell spread area ($n \geq 171$) and focal adhesion area per cell ($n \geq 29$). All data presented as mean ± std; * $p < 0.05$. (For interpretation of the references to color in this figure legend, the reader is referred to the web version of this article.)

nesses similar in range to measurements of fibrosed tissue lead to increases in MF activation as measured by expression of α-SMA, a hallmark of the MF phenotype indicative of heightened contractility [32–39,58,59]. Recently, work by Davidson et al. showed that hepatic stellate cells seeded on hyaluronic acid fibrous matrices expressed higher levels of α-SMA on soft as compared to stiff matrices in the absence of exogenous profibrotic soluble factors, such as TGF-β1 [60]. Additionally, Fiore et al. utilized atomic force microscopy to spatially map stiffness across fibrosing tissue. Interestingly, they found that fibroblastic foci, the region of active fibrogenesis and MF activation, had a low stiffness (E = 1.97 kPa) as compared to mature fibrotic tissue that was much stiffer (E = 8.97 kPa) [61]. These results motivated us to utilize our newly developed DexVS fibrous matrix platform to further investigate the role of matrix stiffness on MF activation in the presence of exogenous profibrotic signals.

NHLFs were cultured at high density for up to a week on soft or stiff DexVS matrices with comparable initial architectural features (i.e. fiber diameter, density, organization). EdU incorporation over the first 24 h of culture and immunostaining for α-SMA expression at day 7 were quantified to assess fibroblast proliferation and activation into MFs, respectively, two hallmarks of fibrotic tissues. In the absence of TGF-β1, negligible α-SMA expression was observed after 7 days of culture (Fig. S5). However, contrary to previous studies using non-fibrous hydrogel surfaces where stiffer substrates induced higher proliferation and MF activation [35–39], we noted the opposite trend: NHLFs in softer, more deformable fibrous matrices with TGF-β1 supplemented media exhibited increased proliferation and MF activation as compared to cells on stiffer matrices with comparable initial architecture (Fig. 8a,b). Along with reorganization of DexVS fibers leading to an increase in tortuosity of the matrix, fibroblasts in soft matrices exhibited α-SMA-enriched

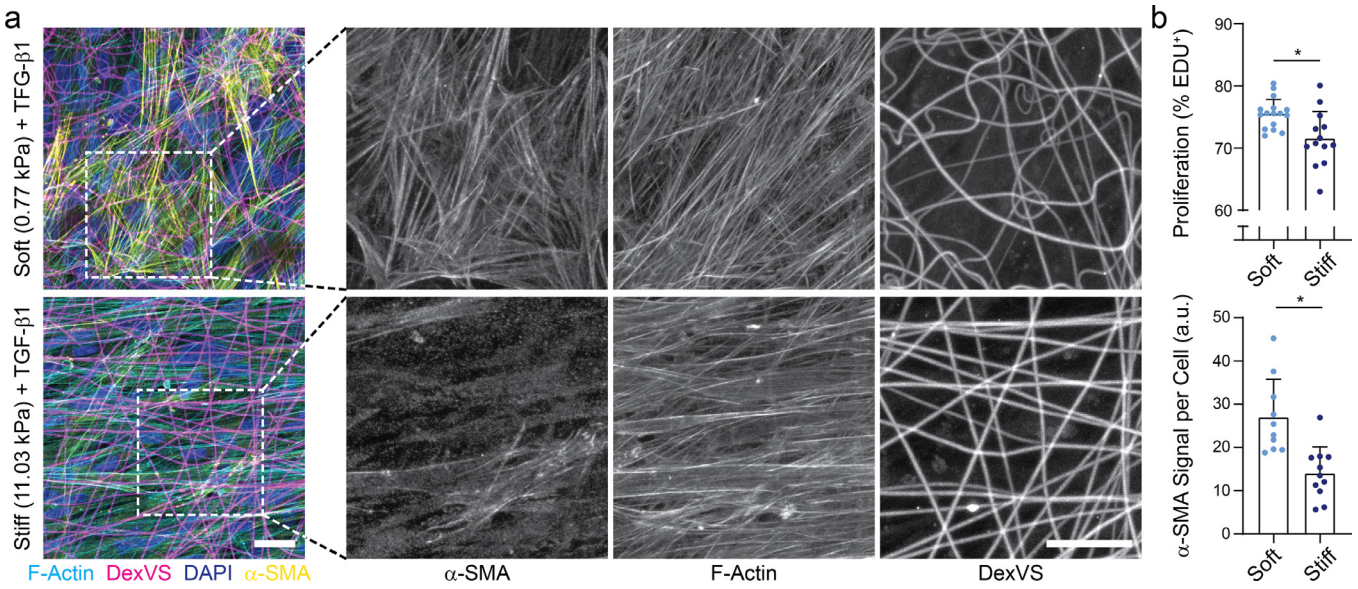

Fig. 8. Soft, deformable DexVS matrices promote MF induction. (a) Confocal fluorescent image of NHLFs cultured for 7 days on soft and stiff DexVS fibrous matrices; F-actin (cyan), DexVS fibers (magenta), nuclei (blue), α-SMA (yellow). Dashed boxes indicate locations of higher magnification images depicting α-SMA stress fibers. (b) Quantification of cell proliferation by EdU labeling ($n \geq 13$) and α-SMA fluorescent intensity ($n \geq 10$). Scale bars: 25 μm. All data presented as mean ± std; * $p \leq 0.05$. (For interpretation of the references to color in this figure legend, the reader is referred to the web version of this article.)

stress fibers (Fig. 8a). Conversely, cells in stiff matrices contained largely cytosolic α-SMA signal and little to no change in matrix structure was noted (Fig. 8a). These data along with previous observations [60,61] interestingly suggest that softer fibrous matrices are permissive to MF activation, while stiffer matrices mechanically similar to fibrosed tissues are not. Indeed, this could in part be explained by densification of matrix fibers seen on soft matrices (Fig. 7b, Fig. 8a), as recent data from our lab has shown that high local fiber densities in 3D promote Yes-associated protein (YAP) activity [62], a transcriptional co-activator required for MF activation [63]. On the contrary, current dogma posits a minimum prerequisite matrix stiffness for MF activation, providing a reinforcement mechanism to this progressive and often irreversible process. These conflicting observations motivate a higher spatiotemporal resolution examination of the matrix and constituent cells during fibrosis, including characterization of matrix porosity, ligand type and density in addition to mechanical stiffness.

4. Conclusion

In this work, we developed a synthetic biomaterial system of electrospun DexVS with tunable mechanics in order to model the fibrous microstructure and mechanical behavior of stromal tissue spaces where disease processes such as fibrosis originate. This system provides tunable and stable mechanical properties at both the single fiber and bulk matrix scale (Fig. 2-4), as well as user-controlled biochemical functionalization with cysteine-terminated cell adhesive peptides (Fig. 5). Alternatively, functionalization with HepMA allows cells to biochemically modify matrices with secreted ECM proteins (Fig. 6). We then used this *in vitro* model of stromal tissue space to investigate MF activation, an important early step in the fibrotic cascade. In contrast to the relationship between matrix stiffness and MF activation established previously on non-fibrous hydrogel substrates, we observed that fibroblasts in soft and deformable fibrous matrices exhibit increased spreading, FA formation, proliferation, and activation into MFs as compared to cells on stiffer matrices with identical initial architecture (Fig. 7,8). This work provides a new user-defined model that recapitulates the fibrous structure of native tissues while enabling cell-mediated physical and biochemical remodeling of the microenvironment. Future efforts to understand the dynamics and reciprocity underlying long-term interactions between cells and matrix will likely be critical to the discovery and development of therapeutics to treat fibrosis.

Declaration of Competing Interest

The authors declare that they have no known competing financial interests or personal relationships that could have appeared to influence the work reported in this paper.

Acknowledgments

C.D.D., D.L.M., and W.Y.W. acknowledge financial support from the National Science Foundation Graduate Research Fellowship Program (DGE1256260). W.Y.W. acknowledges financial support from the University of Michigan Rackham Merit Fellowship. S.J.D. acknoledges financial support from the CELL-MET Engineering Research Center (NSF EEC-1647837). B.M.B. acknowledges financial support from an NIH Pathway to Independence Award (HL124322). We thank the University of Michigan Biointerfaces Institute for the assistance with matrix mechanical testing.

Supplementary materials

Supplementary material associated with this article can be found, in the online version, at doi:10.1016/j.actbio.2020.01.009.

References

[1] V. Vogel, M. Sheetz, Local force and geometry sensing regulate cell functions, Nat. Rev. Mol. Cell Biol. 7 (2006) 265–275.
[2] D.E. Discher, P. Janmey, Y. Wang, Tissue cells feel and respond to the stiffness of their substrate, Science 310 (2005) 1139–1143.
[3] D.E. Ingber, Mechanobiology and diseases of mechanotransduction, Ann. Med. 35 (2003) 564–577.
[4] B. Geiger, J.P. Spatz, A.D. Bershadsky, Environmental sensing through focal adhesions, Nat. Rev. Mol. Cell Biol. 10 (2009) 21–33.
[5] A.D. Bershadsky, N.Q. Balaban, B. Geiger, Adhesion-dependent cell mechanosensitivity, Annu. Rev. Cell Dev. Biol. 19 (2003) 677–695.
[6] B.M. Gumbiner, Cell adhesion: the molecular basis of tissue architecture and morphogenesis, Cell. 84 (1996) 345–357.
[7] A.J. Engler, S. Sen, H.L. Sweeney, D.E. Discher, Matrix elasticity directs stem cell lineage specification, Cell. 126 (2006) 677–689.

[8] E.A. Klein, L. Yin, D. Kothapalli, P. Castagnino, F.J. Byfield, T. Xu, I. Levental, E. Hawthorne, P.A. Janmey, R.K. Assoian, Cell-cycle control by physiological matrix elasticity and in vivo tissue stiffening, Curr. Biol. 19 (2009) 1511–1518.
[9] S. Dupont, L. Morsut, M. Aragona, E. Enzo, S. Giulitti, M. Cordenonsi, F. Zanconato, J. Le Digabel, M. Forcato, S. Bicciato, N. Elvassore, S. Piccolo, Role of YAP/TAZ in mechanotransduction, Nature 474 (2011) 179–184.
[10] F. Guilak, D.M. Cohen, B.T. Estes, J.M. Gimble, W. Liedtke, C.S. Chen, Control of stem cell fate by physical interactions with the extracellular matrix, Cell Stem Cell 5 (2009) 17–26.
[11] K. Kulangara, K.W. Leong, Substrate topography shapes cell function, Soft Matter 5 (2009) 4072–4076.
[12] J. Zeltinger, J.K. Sherwood, D.A. Graham, R. Müeller, L.G. Griffith, Effect of pore size and void fraction on cellular adhesion, proliferation, and matrix deposition, Tissue Eng 7 (2001) 557–572.
[13] O. Chaudhuri, L. Gu, M. Darnell, D. Klumpers, S.A. Bencherif, J.C. Weaver, N. Huebsch, D.J. Mooney, Substrate stress relaxation regulates cell spreading, Nat. Commun. 6 (2015) 1–7.
[14] L. Li, J. Eyckmans, C.S. Chen, Designer biomaterials for mechanobiology, Nat. Mater. 16 (2017) 1164–1168.
[15] R. Parenteau-Bareil, R. Gauvin, F. Berthod, Collagen-based biomaterials for tissue engineering applications, Materials 3 (2010) 1863–1887.
[16] T.A.E. Ahmed, E.V. Dare, M. Hincke, Fibrin: A versatile scaffold for tissue engineering applications, Tissue Eng. Part B Rev. 14 (2008) 199–215.
[17] S. Nakagawa, P. Pawelek, F. Grinnell, Long-term culture of fibroblasts in contracted collagen gels: Effects on cell growth and biosynthetic activity, J. Invest. Dermatol. 93 (1989) 792–798.
[18] E. Kniazeva, A.J. Putnam, Endothelial cell traction and ECM density influence both capillary morphogenesis and maintenance in 3-D, Am. J. Physiol. Cell Physiol. 297 (2009) 179–187.
[19] T.J. Sill, H.A. von Recum, Electrospinning: Applications in drug delivery and tissue engineering, Biomaterials 29 (2008) 1989–2006.
[20] Q.P. Pham, U. Sharma, A.G. Mikos, Electrospinning of polymeric nanofibers for tissue engineering applications: A review, Tissue Eng. 12 (2006) 1197–1211.
[21] R.L. Mauck, B.M. Baker, N.L. Nerurkar, J.A. Burdick, W.-J.J. Li, R.S. Tuan, D.M. Elliott, Engineering on the straight and narrow: The mechanics of nanofibrous assemblies for fiber-reinforced tissue regeneration, Tissue Eng. Part B Rev. 15 (2009) 171–193.
[22] B.M. Baker, B. Trappmann, W.Y. Wang, M.S. Sakar, I.L. Kim, V.B. Shenoy, J.A. Burdick, C.S. Chen, Cell-mediated fibre recruitment drives extracellular matrix mechanosensing in engineered fibrillar microenvironments, Nat. Mater. 14 (2015) 1262–1268.
[23] W.Y. Wang, C.D. Davidson, D. Lin, B.M. Baker, Actomyosin contractility-dependent matrix stretch and recoil induces rapid cell migration, Nat. Commun. 10 (2019) 1186.
[24] C.D. Davidson, W.Y. Wang, I. Zaimi, D.K.P. Jayco, B.M. Baker, Cell force-mediated matrix reorganization underlies multicellular network assembly, Sci. Rep. 9 (2019) 12.
[25] B. Hinz, S.H. Phan, V.J. Thannickal, M. Prunotto, A. Desmoulire, J. Varga, O. De Wever, M. Mareel, G. Gabbiani, Recent developments in myofibroblast biology: Paradigms for connective tissue remodeling, Am. J. Pathol. 180 (2012) 1340–1355.
[26] T.A. Wynn, Common and unique mechanisms regulate fibrosis in various fibroproliferative diseases, J. Clin. Invest. 117 (2007) 524–529.
[27] B. Hinz, G. Celetta, J.J. Tomasek, G. Gabbiani, C. Chaponnier, Alpha-smooth muscle actin expression upregulates fibroblast contractile activity, Mol. Biol. Cell. 12 (2001) 2730–2741.
[28] B. Hinz, S.H. Phan, V.J. Thannickal, A. Galli, M.L. Bochaton-Piallat, G. Gabbiani, The myofibroblast: One function, multiple origins, Am. J. Pathol. 170 (2007) 1807–1816.
[29] I.A. Darby, O. Skalli, G. Gabbiani, α-Smooth muscle actin is transiently expressed by myofibroblasts during experimental wound healing, Lab. Investig. 63 (1990) 21–29.
[30] A.J. Singer, R.A.F. Clark, Cutaneous wound healing, N. Engl. J. Med. 341 (1999) 738–746.
[31] G. Gabbiani, The myofibroblast in wound healing and fibrocontractive diseases, J. Pathol. 200 (2003) 500–503.
[32] B. Hinz, D. Mastrangelo, C.E. Iselin, C. Chaponnier, G. Gabbiani, Mechanical tension controls granulation tissue contractile activity and myofibroblast differentiation, Am. J. Pathol. 159 (2001) 1009–1020.
[33] A. Marinkovic, J.D. Mih, J.A.J.-A. Park, F. Liu, D.J. Tschumperlin, Improved throughput traction microscopy reveals pivotal role for matrix stiffness in fibroblast contractility and TGF- responsiveness, AJP Lung Cell. Mol. Physiol. 303 (2012) 169–180.
[34] P.D. Arora, N. Narani, C.A.G. McCulloch, The compliance of collagen gels regulates transforming growth factor-β induction of α-smooth muscle actin in fibroblasts, Am. J. Pathol. 154 (1999) 871–882.
[35] S.R. Caliari, M. Perepelyuk, B.D. Cosgrove, S.J. Tsai, G.Y. Lee, R.L. Mauck, R.G. Wells, J.A. Burdick, Stiffening hydrogels for investigating the dynamics of hepatic stellate cell mechanotransduction during myofibroblast activation, Sci. Rep. 6 (2016) 1–10.
[36] J.M. Goffin, P. Pittet, G. Csucs, J.W. Lussi, J.J. Meister, B. Hinz, Focal adhesion size controls tension-dependent recruitment of α-smooth muscle actin to stress fibers, J. Cell Biol. 172 (2006) 259–268.
[37] J.A. Benton, B.D. Fairbanks, K.S. Anseth, Characterization of valvular interstitial cell function in three dimensional matrix metalloproteinase degradable PEG hydrogels, Biomaterials 30 (2009) 6593–6603.
[38] H.N. Chia, M. Vigen, A.M. Kasko, Effect of substrate stiffness on pulmonary fibroblast activation by TGF-β, Acta Biomater. 8 (2012) 2602–2611.
[39] J.L. Balestrini, S. Chaudhry, V. Sarrazy, A. Koehler, B. Hinz, The mechanical memory of lung myofibroblasts, Integr. Biol. 4 (2012) 410–421.
[40] Y. Yu, Y. Chau, One-step "click" method for generating vinyl sulfone groups on hydroxyl-containing water-soluble polymers, Biomacromolecules 13 (2012) 937–942.
[41] L. Yang, K.O. Van Der Werf, B.F.J.M. Koopman, V. Subramaniam, M.L. Bennink, P.J. Dijkstra, J. Feijen, Micromechanical bending of single collagen fibrils using atomic force microscopy, J. Biomed. Mater. Res. Part A. 82 (2007) 160–168.
[42] D. Kluge, F. Abraham, S. Schmidt, H.W. Schmidt, A. Fery, Nanomechanical properties of supramolecular self-assembled whiskers determined by AFM force mapping, Langmuir 26 (2010) 3020–3023.
[43] C. Claaßen, A. Southan, J. Grübel, G.E.M. Tovar, K. Borchers, Interactions of methacryloylated gelatin and heparin modulate physico-chemical properties of hydrogels and release of vascular endothelial growth factor, Biomed. Mater. (2018) 13.
[44] G.C.J. Brown, K.S. Lim, B.L. Farrugia, G.J. Hooper, T.B.F. Woodfield, Covalent incorporation of heparin improves chondrogenesis in photocurable gelatin-methacryloyl hydrogels, Macromol. Biosci. 17 (2017) 1–13.
[45] H.M. Borteh, M.D. Gallovic, S. Sharma, K.J. Peine, S. Miao, D.J. Brackman, K. Gregg, Y. Xu, X. Guo, J. Guan, E.M. Bachelder, K.M. Ainslie, Electrospun acetalated dextran scaffolds for temporal release of therapeutics, Langmuir 29 (2013) 7957–7965.
[46] W. Ritcharoen, Y. Thaiying, Y. Saejeng, I. Jangchud, R. Rangkupan, C. Meechaisue, P. Supaphol, Electrospun dextran fibrous membranes, Cellulose 15 (2008) 435–444.
[47] H. Jiang, D. Fang, B.S. Hsiao, B. Chu, W. Chen, Optimization and characterization of dextran membranes prepared by electrospinning, Biomacromolecules 5 (2004) 326–333.
[48] G. Sun, Y.I. Shen, C.C. Ho, S. Kusuma, S. Gerecht, Functional groups affect physical and biological properties of dextran-based hydrogels, J. Biomed. Mater. Res. Part A. 93 (2010) 1080–1090.
[49] J.R. Day, A. David, J. Kim, E.A. Farkash, M. Cascalho, N. Milašinović, A. Shikanov, The impact of functional groups of poly(ethylene glycol) macromers on the physical properties of photo-polymerized hydrogels and the local inflammatory response in the host, Acta Biomater. 67 (2018) 42–52.
[50] M. Guthold, W. Liu, E.A. Sparks, L.M. Jawerth, L. Peng, M. Falvo, R. Superfine, R.R. Hantgan, S.T. Lord, A comparison of the mechanical and structural properties of fibrin fibers with other protein fibers, Cell Biochem. Biophys. 49 (2007) 165–181.
[51] W. Liu, C.R. Carlisle, E.A. Sparks, M. Guthold, The mechanical properties of single fibrin fibers, J. Thromb. Haemost. 8 (2010) 1030–1036.
[52] C. Bonnans, J. Chou, Z. Werb, Remodelling the extracellular matrix in development and disease, Nat. Rev. Mol. Cell Biol. 15 (2014) 786–801.
[53] M.M. Martino, P.S. Briquez, A. Ranga, M.P. Lutolf, J.A. Hubbell, Heparin-binding domain of fibrin(ogen) binds growth factors and promotes tissue repair when incorporated within a synthetic matrix, Proc. Natl. Acad. Sci. U. S. A. 110 (2013) 4563–4568.
[54] J.R. Bishop, M. Schuksz, J.D. Esko, Heparan sulphate proteoglycans fine-tune mammalian physiology, Nature 446 (2007) 1030–1037.
[55] J. Xie, M. Bao, M.C. Bruekers, W.T.S. Huck, Collagen gels with different fibrillar microarchitectures elicit different cellular responses, ACS Appl. Mater. Interfaces. 9 (2017) 19630–19637.
[56] A. Engler, L. Bacakova, C. Newman, A. Hategan, M. Griffin, D. Discher, Substrate compliance versus ligand density in cell on gel responses, Biophys. J. 86 (2004) 617–628.
[57] J.D. Mih, A. Marinkovic, F. Liu, A.S. Sharif, D.J. Tschumperlin, Matrix stiffness reverses the effect of actomyosin tension on cell proliferation, J. Cell Sci. 125 (2012) 5974–5983.
[58] F. Liu, J.D. Mih, B.S. Shea, A.T. Kho, A.S. Sharif, A.M. Tager, D.J. Tschumperlin, Feedback amplification of fibrosis through matrix stiffening and COX-2 suppression, J. Cell Biol. 190 (2010) 693–706.
[59] P.J. Wipff, D.B. Rifkin, J.J. Meister, B. Hinz, Myofibroblast contraction activates latent TGF-β1 from the extracellular matrix, J. Cell Biol. 179 (2007) 1311–1323.
[60] M. Davidson, K. Song, M.H. Lee, J. Llewellyn, Y. Du, B. Baker, R.G. Wells, J.A. Burdick, Engineered fibrous networks to investigate the influence of fiber mechanics on myofibroblast differentiation, ACS Biomater. Sci. Eng. 5 (2019) 3899–3908.
[61] V.F. Fiore, J.S. Hagood, T.H. Barker, V.F. Fiore, S.S. Wong, C. Tran, C. Tan, W. Xu, T. Sulchek, E.S. White, J.S. Hagood, T.H. Barker, $\alpha v\beta 3$ Integrin drives fibroblast contraction and strain stiffening of soft provisional matrix during progressive fibrosis, JCI Insight. 3 (2018).
[62] D.L. Matera, W.Y. Wang, M.R. Smith, A. Shikanov, B.M. Baker, Fiber density modulates cell spreading in 3D interstitial matrix mimetics, ACS Biomater. Sci. Eng. 5 (2019) 2965–2975.
[63] F. Liu, D. Lagares, K.M. Choi, L. Stopfer, A. Marinković, V. Vrbanac, C.K. Probst, S.E. Hiemer, T.H. Sisson, J.C. Horowitz, I.O. Rosas, L.E. Fredenburgh, C. Feghali–Bostwick, X. Varelas, A.M. Tager, D.J. Tschumperlin, Mechanosignaling through YAP and TAZ drives fibroblast activation and fibrosis, Am. J. Physiol. - Lung Cell. Mol. Physiol. 308 (2015) 344–357.